

**Research Article****Effect of solvents and temperature on the structural, thermodynamic and electronic properties of capped phenylalanine: A computational study**

Md. Alauddin*

*Department of Theoretical and Computational Chemistry, University of Dhaka, Dhaka, Bangladesh***ARTICLE INFO****Article History**

Received: 14 September 2021

Revised: 12 November 2021

Accepted: 23 November 2021

Keywords: Capped phenylalanine, DFT, TD-DFT**ABSTRACT**

Effects of solvents and temperature on the structural, thermodynamic, and electronic properties of L-configuration of N-acetyl-phenylalaninyl amide (NAPA) were studied using density functional theory (DFT) and time-dependent density functional theory (TD-DFT) approach. Enthalpy (H), entropy (S) and specific heat capacity (C_v) were found to increase with the increase of temperature (100 K-1600 K) because of the increasing intensities of molecular vibration. On the contrary, Gibb's free energy (G) was found to decrease with the increase of temperature. The UV-light absorption maximum, λ_{max} , is red-shifted in the presence of polar protic, aprotic and non-polar solvents. On the other hand, calculation shows that dipole moment in polar solvents (protic and aprotic), non-polar solvents, and the gas phase are ~3.35, ~3.0, and 2.5 D, respectively. However, no significant change was found in the HOMO-LUMO energy gap in the presence of different types of solvents.

Introduction

Computational studies on biomolecules such as amino acids, peptides, proteins, lipids, nucleic acids etc. have become a promising research area because the objective is to determine the physicochemical properties as well as biological functions directly or indirectly from the structural motifs (Schweitzer-Stenner, 2012; Lanza and Chiacchio, 2013). Due to the flexibility of biomolecules, experimentally, it is not too easy to determine the secondary or tertiary structures of biomolecules (Kolev et al., 2010; Declerck et al., 2019). However, the computational approach, mainly density functional theory (DFT), makes it easy to ascertain the secondary or tertiary structure (Chahkandi and Chahkandi, 2020; Welesa and Broda, 2017; Lanza and Chiacchio, 2014). Recently, a simple peptide with aromatic chromophore became an interesting research topic as it is simpler to determine the secondary structure of

peptides and proteins (Robertson and Simons, 2001; Sobolewski and Domcke, 2006). The originality for the formation of the three-dimensional structure of peptides and proteins mainly occurs from the intramolecular hydrogen bonding (H-bonding) that connects proton donor (NH) and acceptor (CO) amide parts of different residues with the peptide backbone. Based on the connection of donor-acceptor amide sites, many secondary arrangements are formed such as β -strands, γ -turns, β -turns or C_{10} interaction and α -helices or C_{13} interaction (Gerhards et al., 2004; Hunig and Kleinermanns, 2004). Backbone configuration (dihedral angles ϕ and ψ in the Ramachandran plot) are taken into account to identify these structural arrangements depending on the relative orientations of the amide groups (Chin et al., 2005; Richardson, 1981).

*Corresponding author: <alauddin1982@du.ac.bd>

Both left-handed (L) and right-handed (D) enantiomeric proteins are found in nature, but most of the natural proteins have left-handed (L) configurations (Goodman and Gershwin, 2006; Rose et al., 1985). Therefore, the researchers are always interested in working on peptides consisting of L-amino acids. N-acetyl-phenylalaninyl amide (NAPA) is a simple dipeptide used to analyze intra- and intermolecular interactions within the back-bone chain of the protein. Additionally, the presence of aromatic side-chain in NAPA shows intense photophysics in the spectral range of ultra-violet (UV) (Malis et al., 2014; Molis et al., 2012).

An important matter regarding the stability of the secondary structures of peptide and protein involves the effect of solvents (polar protic, polar aprotic, and non-polar solvents). It is well established that both explicit and implicit solvent effects have a key role in stabilizing the charged peptides due to strong ion-dipole and hydrogen bonding interactions. However, the magnitude of these interactions is prominently lessened for the neutral systems (Mullin and Gordon, 2009). Another important issue for the structures of peptides and proteins concerns the effect of temperature. Several independent research works have been conducted on peptides to understand the secondary equilibrium structure (Toal et al., 2014; Hong et al., 2013; Lanza and Chiacchio, 2014).

Lanza and Chiacchio reported for AcXxxNH₂ and AcXxxNHCH₃ (Xxx= Gly, Ala, and Leu) model peptides with left-handed polyproline II (PPII) helix at room temperature. However, the quantity of β -strand increases rapidly and becomes prominent with increasing of temperature. This shows that the PPII structural motif is enthalpically favored, whereas β -strand structure is stabilized by entropy. A recent DFT and TDDFT study of the structural, thermodynamic, spectroscopic, and electronic properties of capped

phenylalanine has been reported (Alauddin, 2021). In this paper, the results of an investigation of the structural motif of NAPA and the effect of solvents and temperature on the thermodynamic stability and electronic properties of NAPA-A are reported.

Methods and Materials

Computational details

The conformers of the NAPA compound analyzed herein were initially explored using the AMBER force field (Case et al., 2006) included in the Hyper Chem professional 7.51 package (Hyper Chem Professional 7.51, 2002). Geometry optimization of NAPA was performed using Gaussian16 computational package (Frisch et al., 2016), and *Gauss View* 6.0 were used to visualize the molecular geometry. The analysis of vibrational modes was performed on the optimized structures to evaluate the nature of stationary points and to get zero-point vibration energy (ZPVE). No imaginary frequencies were obtained, which confirm the minimum energy structure. All the quantum chemical calculations were performed by DFT method combined with dispersion correction functional (*w*B97XD) using the more accurate basis set of cc-pVTZ in the gas phase. On the other hand, to see the effects of various solvents, implicit solvent effects were modeled using the integral equation formalism variant polarizable continuum model (IEF-PCM) as implemented in the Gaussian16 program. The UV-Visible spectra, and the electronic properties like frontier molecular orbitals (HOMO, highest occupied molecular orbitals and LUMO, lowest unoccupied molecular orbital) were calculated with the aid of the time-dependent density functional theory (TD-DFT) approach. The absorption maxima, oscillator strength, HOMO energy, LUMO, and HOMO-LUMO energy gap were identified with the help of Gauss-Sum 3.0 software (O'boyle et al., 2008).

Results and Discussion

Optimized molecular geometry

After conformational explorations of the L-configuration of NAPA, several conformers were optimized with DFT/wB97XD/cc-p VTZ computational approach. Finally, we found the four most stable conformers of NAPA depending on the result on backbone dihedral angles (φ_c , ψ_N) and the orientation of the phenyl ring (χ_1). They are assigned as NAPA-A, NAPA-B, NAPA-C and NAPA-D with structural motifs of $\beta_L(a)$, $\gamma_L(g+)$, $\gamma_L(g-)$ and $\gamma_L(a)$, respectively, characterized by Ramachandran angles. The four most stable conformers of NAPA are shown in Fig. 1 with their structural motifs. The conformations are assigned gauche (g^\pm) if the χ_1 dihedral angle lies between 0 and $\pm 120^\circ$ and anti (a) otherwise (Chin et al., 2004).

The computed φ_c , ψ_N , and χ_1 dihedral angles of NAPA-A, NAPA-B, NAPA-C, and NAPA-D conformers are shown in Table 1.

NAPA-D with structural motifs of $\beta_L(a)$, $\gamma_L(g+)$, NAPA-A is the extended backbone form with weak intramolecular C_5 hydrogen-bonding interaction as well as $NH \cdots \pi$ interaction. The Ramachandran angles (φ_c , ψ_N) of NAPA-A are -158.89° and $+163.80^\circ$ that identify the $\beta_L(a)$ structural motif. The φ_c , ψ_N and χ_1 dihedral angles of NAPA-B are -82.97° , $+53.84^\circ$ and $+42.84^\circ$, respectively that determine $\gamma_L(g+)$ structural motif of NAPA-B. NAPA-C and NAPA-D have the structural assignments of $\gamma_L(g-)$ and $\gamma_L(a)$ according to Ramachandran dihedral angles and phenyl side-chain angle.

Table 1. Comparison of backbone dihedral angles (φ_c , ψ_N) and phenyl side-chain dihedral angle (χ_1) for the DFT-optimized most stable conformers of NAPA-A, NAPA-B NAPA-C and NAPA-D with their structural motifs.

Conformer	Type of angle	Dihedral angle	In egre ($^\circ$)	Structural Motifs
NAPA-A	Ramachandran angles (Backbone angles)	$\varphi_c = (C18-N16-C1-C24)$ $\psi_N = (N16-C1-C24-N26)$	-158.89 $+163.80$	$\beta_L(a)$, E, Weak C_5 Interaction
	Phenyl side-chain angle	$\chi_1 = (N16-C1-C2-C3)$	-164.31	
	Ramachandran angles (Backbone angles)	$\varphi_c = (C13-N7-C1-C3)$ $\psi_N = (N7-C1-C3-N9)$	-82.97 $+53.84$	
Phenyl side-chain angle	$\chi_1 = (N7-C1-C2-C4)$	$+42.84$		
NAPA-C	Ramachandran angles (Backbone angles)	$\varphi_c = (C13-N7-C1-C3)$ $\psi_N = (N7-C1-C3-N9)$	-86.13 $+70.59$	$\gamma_L(g-)$, FC_7 Interaction
	Phenyl side-chain angle	$\chi_1 = (N7-C1-C2-C4)$	-55.53	
	Ramachandran angles (Backbone angles)	$\varphi_c = (C13-N7-C1-C3)$ $\psi_N = (N7-C1-C3-N9)$	-83.54 $+81.76$	
Phenyl side-chain angle	$\chi_1 = (N7-C1-C2-C4)$	-165.98		

E= Extended, F^L = folded with L conformer, a = anti-, g+ = gauche+, g- = gauche-

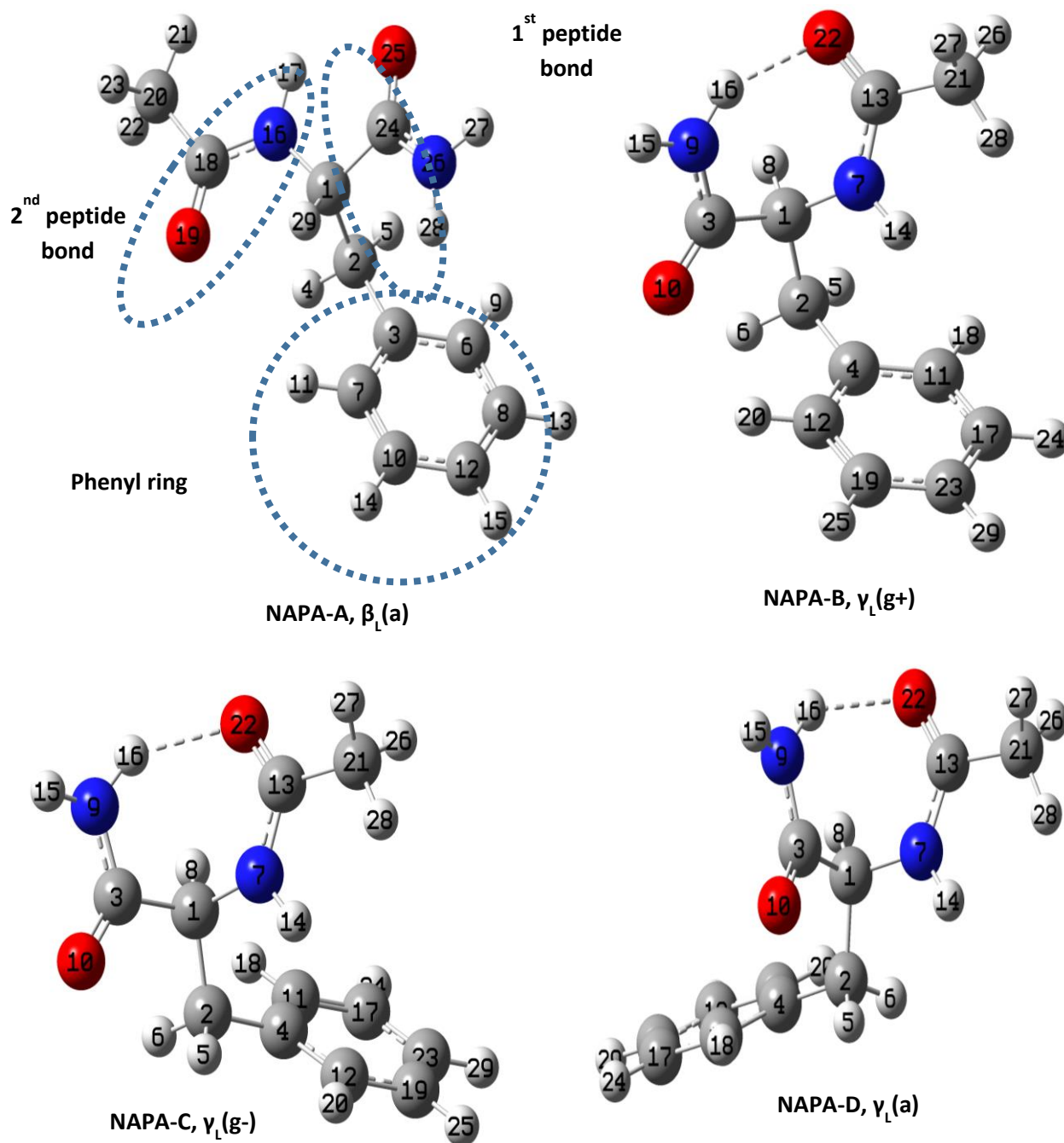


Fig. 1. The four most stable conformers of NAPA in the gas phase were computed at the DFT/*w*B97XD/cc-pVTZ level of theory. The structural motifs of conformer A, B, C, and D are $\beta_L(a)$, $\gamma_L(g+)$, $\gamma_L(g-)$ and $\gamma_L(a)$, respectively. Labels *g±* and *a* refer to the orientation of the phenyl side chain relative to the backbone

Thermodynamics parameters at different temperatures

The effect of temperature on the thermodynamic parameters was computed using Gaussian 16.0 program package where temperature and pressure are 298.15 K and 1 atmosphere, respectively, by default. Gibb's free energy (G), enthalpy (H), entropy (S), specific heat capacity (C_v), electronic energy (Hartree), and polarizability (α) were calculated in the region of 100 K to 1600 K to quantify the effect of temperature and displayed in Table 2. The first four thermodynamic parameters for the NAPA molecule correlate well with the temperature showing graphs as represented in Fig. 2.

The correlation fitting equation among changes in G, H, S, and C_v with temperature was fitted by quadratic formulas, and the fitting equations with regression factors (R^2) are derived using Origin 16 software. The thermodynamic correlation fitting equations are

$$G = 156.91093 - 0.09091T - 7.04468 \times E^{-5}T^2$$

$$(R^2 = 0.99988)$$

$$H = 145.40783 + 0.0468T + 3.71738 \times E^{-5}T^2$$

$$(R^2 = 0.99912)$$

$$S = 64.67097 + 0.21404T - 4.2222 \times E^{-5}T^2$$

$$(R^2 = 0.99986)$$

$$C_v = 7.99294 + 0.17585T - 5.79716 \times E^{-5}T^2$$

$$(R^2 = 0.99711)$$

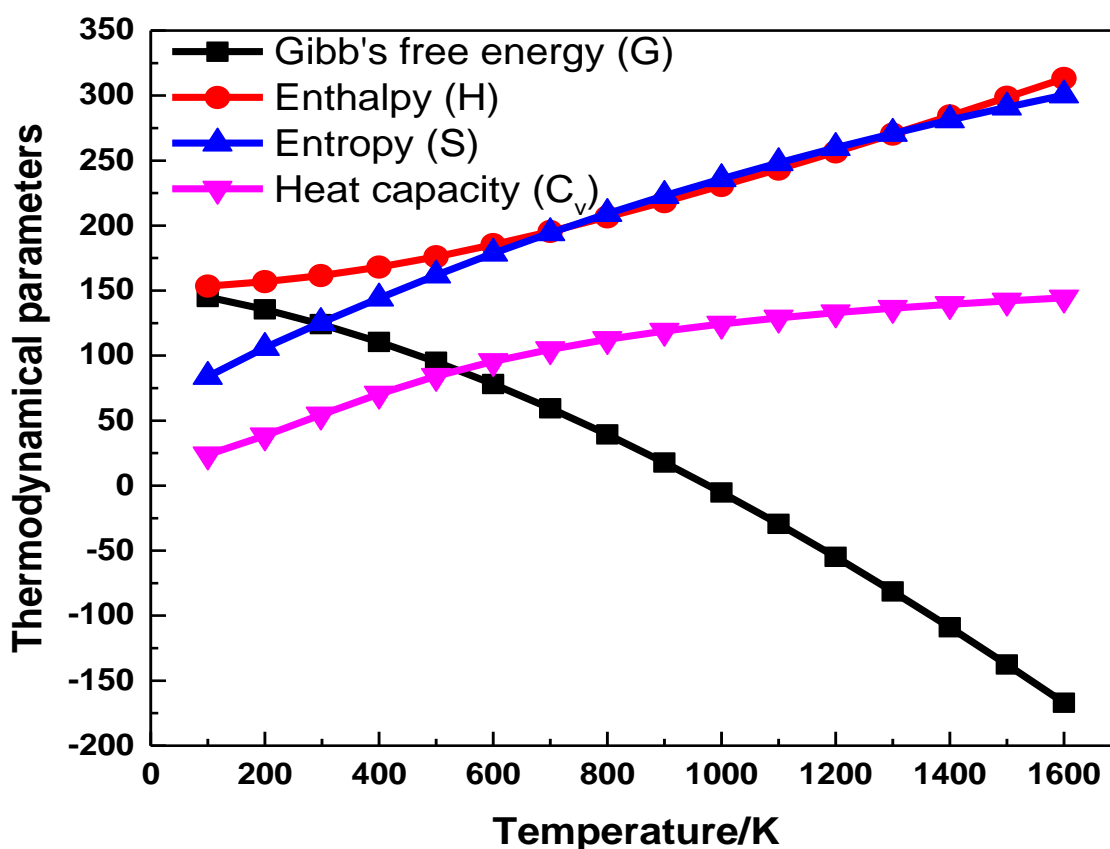


Fig. 2. Graphs representing the dependency of Gibb's free energy (G), enthalpy (H), entropy (S), and specific heat capacity (C_v) at different temperatures (100K-1600K) for the most stable conformer of NAPA (NAPA-A).

Table 2. Temperature dependence selected thermodynamic parameters of NAPA calculated at the DFT/*w*B97XD/cc-pVTZ level of theory.

Temp. /K	Gibb's free energy, G (kcal/mol)	Enthalpy, H (kcal/mol)	Entropy, S (cal/mol-Kelvin)	Specific heat capacity, Cv (cal/mol-Kelvin)	Electronic Energy, E (Hartree) zpve corr.	Polarizability, α (a.u)
100	145.109	153.499	83.898	23.822	-687.38286	140.770
200	135.563	156.795	106.163	38.474	-687.38286	140.770
298.15	124.195	161.542	125.263	54.414	-687.38286	140.770
400	110.470	168.121	144.130	70.545	-687.38286	140.770
500	95.165	176.080	161.834	84.255	-687.38286	140.770
600	78.136	185.288	178.590	95.543	-687.38286	140.770
700	59.481	195.518	194.341	104.783	-687.38286	140.770
800	39.300	206.589	209.113	112.432	-687.38286	140.770
900	17.689	218.361	222.971	118.855	-687.38286	140.770
1000	-5.265	230.725	235.993	124.308	-687.38286	140.770
1100	-29.460	243.399	248.255	128.977	-687.38286	140.770
1200	-54.849	256.691	259.827	132.997	-687.38286	140.770
1300	-81.362	270.356	270.772	136.474	-687.38286	140.770
1400	-108.940	284.345	281.146	139.493	-687.38286	140.770
1500	-137.529	298.616	290.999	142.124	-687.38286	140.770
1600	-167.077	313.133	300.375	144.424	-687.38286	140.770

It is observed from the related figure and table that the enthalpy rises slowly in the range of low temperature and rises more steeply in the range of high temperature. Only translation parts of motion contribute at low temperatures, but rotational and vibrational motions are excited as temperature increases. On the other hand, the change of entropy increases rapidly with respect to temperature due to the equipartition of energy. That means the thermal energy is distributed rapidly to the translational, rotational, and vibrational modes. The change of specific heat capacity increases gradually at low temperatures and gradually reaches a plateau in the higher temperature region. This indicates that above a certain temperature (>1000K), molecular motion is not increased, and henceforth specific heat capacity becomes almost constant. Another important thermodynamic parameter is Gibb's free energy that decreases with temperature rise. Since the change in Gibb's free energy (G) depends on $-T\Delta S$, (minus temperature (T) times the change in entropy (S)), it decreases as the entropy increases with the increase of temperature.

Electronic excitation of NAPA-A in gas and different solvents

The TD-DFT calculation is the most efficient and commonly utilized method to predict molecules' electronic transition, allowing for the best compromise of the high level of accuracy and low computational cost. In the gas phase, the six lowest singlet excited states were calculated using TD-DFT/*w*B97XD/cc-pVTZ computational method. Different types of solvents such as polar protic solvents (water (H_2O) and methanol (CH_3OH)), polar aprotic solvents (dichloromethane (DCM), tetrahydrofuran (THF), acetonitrile (CH_3CN) and dimethyl sulfoxide (DMSO)) and non-polar solvents (benzene (C_6H_6), chlorobenzene (C_6H_5Cl), toluene ($C_6H_5CH_3$) and chloroform ($CHCl_3$)) were chosen to reveal the effect of environmental polarity on frontier molecular orbitals (HOMO and LUMO) and electronic absorption spectra. The optical properties, stability, and chemical reactivity of a molecule

strongly depend on the bandgap energy between HOMO and LUMO (Alturk *et al.*, 2018). Another important property to explore the solvation effect is the molecular dipole moment. It is well-known that the magnitude of molecular dipole moment in the solvent phase is larger compared to the gas phase. It also depends on the polarity of solvents (Kosar and Albayrak, 2011). The absorption maxima (λ_{max}), oscillator strengths (f), the energy of HOMO and LUMO, HOMO-LUMO energy gap, molecular dipole moment (μ), global hardness (η), softness (S) and electrophilicity index (ω) of NAPA-A at various solvents were calculated with TD-DFT/*w*B97XD/cc-pVTZ computational method using IEF-PCM model. The computed data obtained in different types of solvents having different polarities are presented in Table 3.

The calculated UV-Visible absorption spectra of NAPA-A in gas and different solvents are exhibited in Fig. 3. The absorption maximum (λ_{max}) was found at 180.25 nm (6.879 eV) with the oscillator strength of 0.4816 in the gas phase. This is a local excitation (LE) with the nature of the electronic transition from π to π^* (Malis *et al.*, 2014). On the other hand, λ_{max} was found at around 182 nm (6.813 eV) for polar protic, aprotic, and non-polar solvents. This indicates that solvation reduces the excitation energies and induces redshift in the electronic spectrum. Although the red-shift is not so large, oscillator strength (f) was enhanced significantly for the solvation. On the other hand, TDDFT-calculated results show that the polarity of solvents has little effect on the energy of frontier orbitals and the HOMO-LUMO energy gap.

The HOMO-LUMO energy distribution for NAPA-A at various solvents is shown in Fig.4. It is found that oscillator strength enhanced significantly and almost same magnitude by protic, aprotic and non-polar solvents. Normally, the molecular dipole moment in the gas phase is lower compared to the solvent phase. Our calculation shows that dipole moment values in polar solvents (protic and aprotic),

Table 3. DFT calculated absorption maxima (λ_{\max}), oscillator strength (f), the energy of HOMO(H), LUMO (L), HOMO-LUMO (H-L) gap, dipole moment (μ), global hardness (η), softness (S), and electrophilicity index (ω) of NAPA-A at various solvents.

Types of solvents	Name of Solvents	λ_{\max} /nm	f	E. of HOMO /eV	E. of LUMO /eV	H-L gap /eV	μ/D	η/eV	S/eV	ω/eV
Polar protic	Gas	180.25	0.4816	-8.90	1.24	10.14	2.578	5.070	0.0986	1.447
	CH ₃ OH	181.52	0.8452	-8.90	1.30	10.20	3.379	5.100	0.0980	1.416
	H ₂ O	181.53	0.8496	-8.90	1.30	10.20	3.411	5.100	0.0980	1.416
Polar aprotic	CH ₃ CN	181.62	0.8538	-8.90	1.30	10.20	3.384	5.100	0.0980	1.416
	THF	182.09	0.8745	-8.89	1.30	10.19	3.220	5.095	0.0981	1.413
	DCM	182.18	0.8856	-8.89	1.30	10.19	3.252	5.095	0.0981	1.413
	DMSO	182.05	0.8905	-8.90	1.30	10.20	3.396	5.100	0.0980	1.416
Non-polar	CHCl ₃	182.39	0.8873	-8.89	1.29	10.18	3.124	5.090	0.0982	1.418
	C ₆ H ₅ CH ₃	182.83	0.8936	-8.89	1.28	10.17	2.922	5.085	0.0983	1.424
	C ₆ H ₆	182.87	0.8944	-8.89	1.28	10.17	2.906	5.085	0.0983	1.424
	C ₆ H ₅ Cl	182.78	0.9231	-8.89	1.30	10.19	3.168	5.095	0.0981	1.413

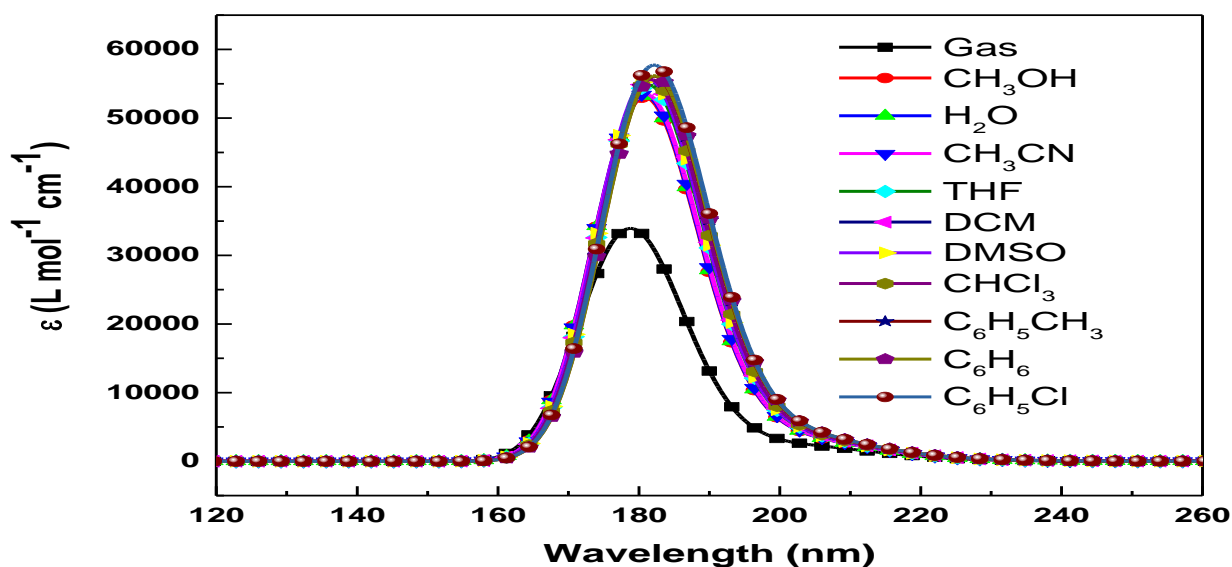


Fig. 3. DFT-calculated UV spectra of the most stable conformer of NAPA (NAPA-A) at various solvents (polar protic, aprotic and non-polar solvents).

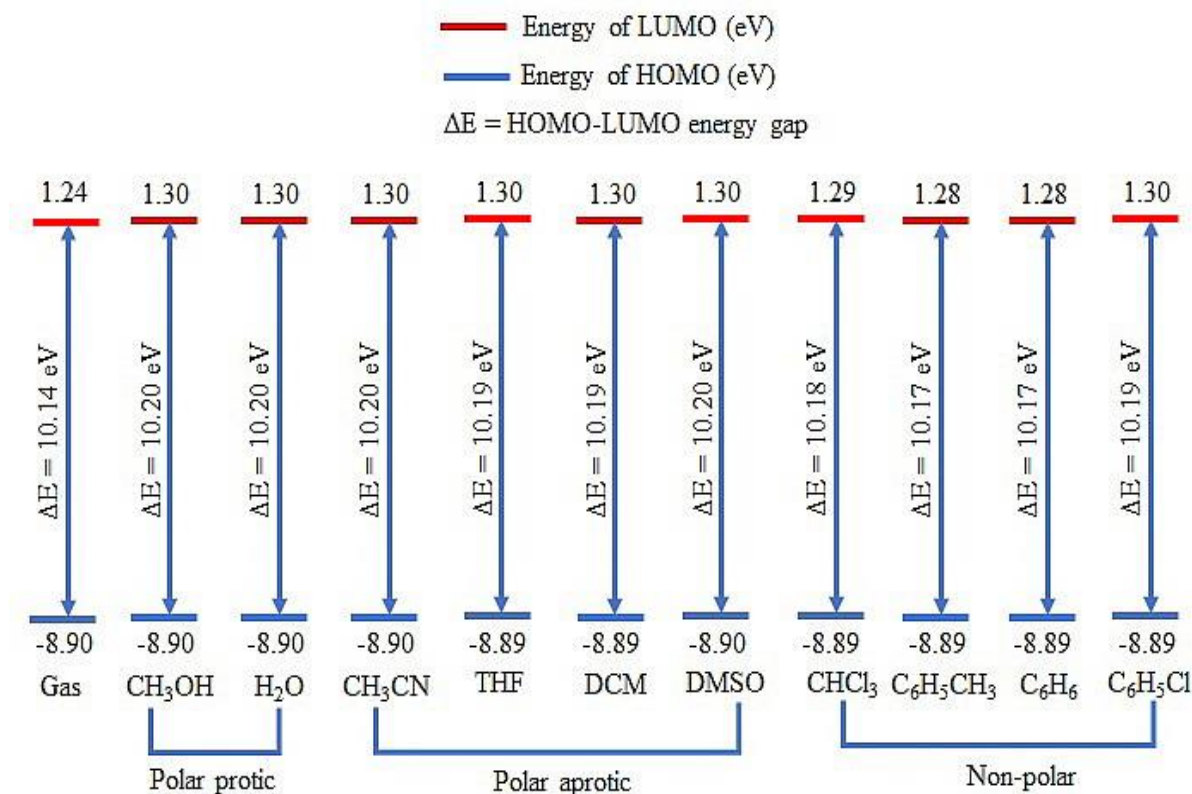


Fig. 4. The HOMO-LUMO energy distribution plot for the most stable conformer of NAPA (NAPA-A) at various solvents (polar protic, aprotic, and non-polar solvents).

non-polar solvents and gas are ~ 3.35 , ~ 3.0 , and 2.5 D, respectively. This indicates that dipole moment increased more by polar solvents, either protic or aprotic than non-polar solvents because charge delocalization increases due to the presence of polar solvents and therefore induces an increase in dipole moments (Kosar and Albayrak, 2011).

Conclusion

DFT and TD-DFT computational approaches combined with dispersion correction functional ($wB97XD$) using a basis set of $cc-pVTZ$ were utilized to understand the effects of solvents and temperature on the structural, thermodynamic and electronic properties of NAPA-A. The minimum energy conformer of NAPA is an extended form with the structural motif of $\beta_L(a)$ in the gas phase. On the other hand, implicit solvent modeling was done using IEF-PCM to see the effects of solvents. Selected

thermodynamic parameters such as enthalpy (H), entropy (S), and specific heat capacity (C_v) were found to increase with the increase of temperature (100 K-1600 K) as the intensities of molecular vibration increases with temperature. However, Gibb's free energy (G) gradually decreases because it depends on entropy. The absorption maxima, λ_{max} , found at around 182 nm (6.813 eV) for polar protic, aprotic, and non-polar solvents whereas 180.25nm (6.879 eV) in the gas phase. This calculation indicates solvation reduces the excitation energies and induces redshift in the electronic spectrum. Interestingly, the red-shift is not too much, but oscillator strength (f) was enhanced significantly for the solvation. Calculation of excited state showed that polarity of solvents has little effect on the energy of frontier orbitals and HOMO-LUMO energy gap. However, oscillator strength was enhanced significantly and almost by the same magnitude by protic, aprotic, and non-polar solvents. Finally,

dipole moment calculation showed that it is increased more by polar solvents, either protic or aprotic compared to non-polar solvents.

Conflicts of Interest

The author declare that there is no conflicts of interest, financial or otherwise.

References

- Alauddin M. DFT and TDDFT studies of structural, thermodynamic, spectroscopic and electronic properties of capped phenylalanine; *J. Bangladesh. Chem. Soc.* 2021; 33(1), 33-39.
- Alturk S, Avci D, Tamer O and Atalay Y. ¹H-pyrazole-3-carboxylic acid: Experimental and computational study. *J. Mol. Struct.* 2018; 1164: 28-36.
- Case DA, Darden T, Cheatham T and Simmerling C. AMBER 9, University of California: San Francisco, 2006.
- Chahkandi B and Chahkandi M. A reconnaissance DFT study of the full conformational analysis of N-formyl-L-serine-L-alanine-NH₂ dipeptide. *J. Mol. Model.* 2020; 26: 151-162.
- Chin W, Dognon JP, Piuzzi F, Tardivel B, Dimicoli I and Mons M. Intrinsic folding of small peptide chains: spectroscopic evidence for the formation of α -turns in the gas phase. *J. Am. Chem. Soc.* 2005; 127: 707-712.
- Chin W, Mons M, Dognon JP, Piuzzi F, Tardivel B and Dimicoli I. Competition between local conformational preferences and secondary structures in gas-phase model tripeptides as revealed by laser spectroscopy and theoretical chemistry. *Phys. Chem. Chem. Phys.* 2004; 6: 2700-2709.
- Declerck V, Perez-Mellor A, Guillot R, Aitken DJ, Mons M and Zehnacker A. Vibrational circular dichroism as a probe of solid-state organisation of derivatives of cyclic β -amino acids: Cis-and trans-2-aminocyclobutane-1-carboxylic acid. *Chirality* 2019; 31: 547-560.
- Frisch MJ, Trucks GW, Schlegel HB, Scuseria GE, Robb MA, Cheeseman JR, Scalmani G, Barone V, Petersson GA, Nakatsuji H, Li X, Caricato M, Marenich AV, Bloino J, Janesko BG, Gomperts R, Mennucci B, Hratchian HP, Ortiz JV, Izmaylov AF, Sonnenberg JL, Williams-Young D, Ding F, Lipparini F, Egidi F, Goings J, Peng B, Petrone A, Henderson T, Ranasinghe D, Zakrzewski VG, Gao J, Rega N, Zheng G, Liang W, Hada M, Ehara M, Toyota K, Fukuda R, Hasegawa J, Ishida M, Nakajima T, Honda Y, Kitao O, Nakai H, Vreven T, Throssell K, Montgomery JA, Peralta JE, Ogliaro F, Bearpark MJ, Heyd JJ, Brothers EN, Kudin KN, Staroverov VN, Keith TA, Kobayashi R, Normand J, Raghavachari K, Rendell AP, Burant JC, Iyengar SS, Tomasi J, Cossi M, Millam JM, Klene M, Adamo C, Cammi R, Ochterski JW, Martin RL, Morokuma K, Farkas O, Foresman JB and Fox DJ Gaussian 16, Revision B.01. Gaussian, Inc., Wallingford, 2016.
- Gerhards M, Unterberg C, Gerlach A and Jansen A. β -sheet model systems in the gas phase: Structures and vibrations of Ac-Phe-NHMe and its dimer (Ac-Phe-NHMe)₂. *Phys. Chem. Chem. Phys.* 2004; 6: 2682-2690.
- Goodman G and Gershwin ME. The origin of life and the left-handed amino-acid excess: The furthest heavens and the deepest seas? *Expt. Bio. Med.* 2006; 231: 1587-1592.
- Hong Z, Wert J and Asher SA. UV Resonance Raman and DFT studies of arginine side chains in peptides: insights into arginine hydration. *J. Phys. Chem. B* 2013; 117: 7145 -7156.
- Hunig I and Kleinermanns K. Conformers of the peptides glycine-tryptophan, tryptophan-glycine and tryptophan-glycine-glycine as revealed by double resonance laser spectroscopy. *Phys. Chem. Chem. Phys.* 2004; 6: 2650-2658.
- Hyper Chem Professional 7.51; Hypercube, Inc.: Gainesville, FL, 2002.
- Kolev T, Spitteller M and Koleva B. Spectroscopic and structural elucidation of amino acid derivatives and small peptides: experimental and theoretical tools. *Amino Acids*, 2010; 38: 45-50.
- Kosar B and Albayrak C. Spectroscopic investigations and quantum chemical computational study of (E)-4-methoxy-2-[(p-tolylimino)methyl]phenol. *Spectrochim. Acta A* 2011; 78: 160-167.

- Lanza G and Chiacchio MA. Comprehensive and accurate *ab initio* energy surface of simple alanine peptides. *Chem. Phys. Chem.* 2013; 14(14): 3284-3293.
- Lanza G and Chiacchio MA. *Ab initio* MP2 and density functional theory computational study of AcAlaNH₂ peptide hydration: A bottom-up approach. *Chem. Phys. Chem.* 2014; 15: 2785-2793.
- Malis M, Loquais Y, Gloaguen E, Jouvét C, Brenner V, Mons M, Ljubic I and Doslic N. Non-radiative relaxation of UV photo excited phenylalanine residues: probing the role of conical intersections by chemical substitution. *Phys. Chem. Chem. Phys.* 2014; 16: 2285-2288.
- Malis M, Loquais Y, Gloaguen E, Biswal HS, PiuZZi F, Tardivel B, Brenner V, Broquier M, Jouvét C, Mons M, Doslic N and Ljubic I. Unraveling the mechanisms of nonradiative deactivation in model peptides following photo excitation of a phenylalanine residue. *J. Am. Chem. Soc.* 2012; 134: 20340-20351.
- Mullin JM and Gordon MS. Alanine: Then there was water. *J. Phys. Chem. B* 2009; 113 (25): 8657-8669.
- O'boyle NM, Tenderholt AL and Langner KM. cclib: A library for package-independent computational chemistry algorithms. *J. Comp. Chem.* 2008; 29(5): 839-845.
- Richardson JS. The anatomy and taxonomy of protein structure. *Adv. Protein Chem.* 1981; 34: 167-339.
- Robertson EG and Simons JP. Getting into shape: Conformational and supramolecular landscapes in small biomolecules and their hydrated clusters. *Phys. Chem. Chem. Phys.* 2001; 3: 1-18.
- Rose GD, Gierasch LM and Smith JA. Turns in peptides and proteins. *Adv. Protein Chem.* 1985; 37: 1-109. Schweitzer-Stenner R.
- Schweitzer-Stenner R. Protein and peptide folding, misfolding and non-folding Hoboken: John Wiley & Sons, Inc. 2012
- Sobolewski AL and Domcke W. Relevance of electron-driven proton-transfer processes for the photo stability of proteins. *Chem. Phys. Chem.* 2006; 7: 561-564.
- Toal SE, Verbaro DJ and Schweitzer-Stenner R. Role of enthalpy-entropy compensation interactions in determining the conformational propensities of amino acid residues in unfolded peptides. *J. Phys. Chem. B* 2014; 118: 1309 -1318.
- Walesa R and Broda MA. The influence of solvent on conformational properties of peptides with Aib residue-a DFT study. *J. Mol. Model.* 2017; 23: 349.